Pharm Res (2015) 32:1727–1740
DOI 10.1007/s11095-014-1571-4

RESEARCH PAPER

Self Assembled Ionically Sodium Alginate Cross-Linked Amphotericin B Encapsulated Glycol Chitosan Stearate Nanoparticles: Applicability in Better Chemotherapy and Non-Toxic Delivery in Visceral Leishmaniasis

Pramod K. Gupta • Anil K. Jaiswal • Shalini Asthana • Ashwni Verma • Vivek Kumar • Prashant Shukla • Pankaj Dwivedi • Anuradha Dube • Prabhat R. Mishra

Received: 3 July 2014 / Accepted: 10 November 2014 / Published online: 26 November 2014

ABSTRACT

Objectives To investigate the applicability, localization, biodistribution and toxicity of self assembled ionically sodium alginate cross-linked AmB loaded glycol chitosan stearate nanoparticles for effective management of visceral leishmaniasis.

Methods Here, we fabricated Amphotericin B (AmB) encapsulated sodium alginate-glycol chitosan stearate nanoparticles (AmB-SA-GCS-NP) using strong electrostatic interaction between oppositely charged polymer and copolymer by ionotropic complexation method. The tagged FAmB-SA-GCS-NP was compared with tagged FAmB for *in vitro* macrophagic uptake in J774A macrophages and *in vivo* localization in liver, spleen, lung and kidney tissues. The AmB-SA-GCS-NP and plain AmB were compared for *in vitro* and *in vivo* antileishmanial activity, pharmacokinetics, organ distribution and toxicity profiling.

Results The morphology of SA-GCS-NP revealed as nanocrystal (size, 196.3 ± 17.2 nm; PDI, 0.216 ± 0.078; zeta potential, (−) 32.4 ± 5.1 mV) by field emission scanning electron microscopy and high resolution transmission electron microscopy. The macrophage uptake and *in vivo* tissue localization studies shows tagged FAmB-SA-GCS-NP has significantly higher (~1.7) uptake compared to tagged FAmB. The biodistribution study of AmB-SA-GCS-NP showed more localized distribution towards *Leishmania* infected organs *i.e.* spleen and liver while lesser towards kidney. The *in vitro* (IC_{50}, 0.128 ± 0.024 μg AmB/ml) and *in vivo* (parasite inhibition, 70.21 ± 3.46%) results of AmB-SA-GCS-NP illustrated significantly higher ($P < 0.05$) efficacy over plain AmB. The monomeric form of AmB within SA-GCS-NP, observed by UV-visible spectroscopy, favored very less *in vitro* and *in vivo* toxicities compared to plain AmB.

Conclusion The molecular organization, toxicity studies, desired localization and biodistribution of cost effective AmB-SA-GCS-NP was found to be highly effective and can be proved as practical delivery platform for better management of leishmaniasis.

KEY WORDS glycol chitosan · molecular organization · stearic acid · sodium alginate · tissue localization · toxicity

Electronic supplementary material The online version of this article (doi:10.1007/s11095-014-1571-4) contains supplementary material, which is available to authorized users.

P. K. Gupta · S. Asthana · A. Verma · V. Kumar · P. Shukla · P. Dwivedi · P. R. Mishra (✉)
Pharmaceutics Division, Preclinical South PCS 002/011
CSIR-Central Drug Research Institute B.S. 10/1, Sector-10, Jankipuram Extension, Sitapur Road, Lucknow 226031, India
e-mail: mishrapr@hotmail.com

P. R. Mishra
e-mail: prabhat_mishra@cdri.res.in

P. K. Gupta
e-mail: pramodcdri10@gmail.com

S. Asthana
e-mail: asthanashalini470@gmail.com

A. Verma
e-mail: ashwni.verma@gmail.com

V. Kumar
e-mail: pvivek.cdri@gmail.com

P. Shukla
e-mail: prashuklaitbhu@gmail.com

P. Dwivedi
e-mail: dwivedipank@gmail.com

A. K. Jaiswal · A. Dube
Parasitology Division CSIR-Central Drug Research Institute, B 10/1, Sector 10, Jankipuram Extension, Sitapur Road, Lucknow 226031, India

A. K. Jaiswal
e-mail: aniljaiswal4@gmail.com

A. Dube
e-mail: anuradha_dube@hotmail.com

INTRODUCTION

Leishmania spp. are obligatory intracellular parasites of macrophages that cause a wide range of human diseases, diffuse cutaneous leishmaniasis, including self-healing skin lesions, localized cutaneous leishmaniasis (CL), mucosal leishmaniasis (ML), and visceral leishmaniasis (VL). The recovery and resistance to all forms of disease are completely dependent on T-cell responses [1].

Glycol chitosan (GC) is commercially available, water soluble derivative of bio-compatible and bio-degradable natural polymer chitosan and has been used as a scaffold for drug delivery [2]. Stearic acid has long acyl chain that provides stronger interaction between copolymer and AmB, responsible for more sustained release for intercalated Amphotericin B (AmB) and, it prevents self-association of AmB molecules and shows reduced drug related toxicity [3]. The glycol chitosan-stearate (GCS) copolymer was synthesized [4] that are known to form self assembled structure [5]. Previously our group investigated that sodium alginate (SA), a natural polysaccharide, induces cytokine release, and initiate activation of innate immune system through activation of macrophage like cells [6,7].

In continuation to this, a polyion complex (PIC) can be easily formed when oppositely charged polyelectrolytes are mixed in aqueous solution and interact *via* electrostatic interactions. Various nanostructures such as nanoparticles, nanogels and hollow nanospheres composed of PIC are prepared by altering formulation parameters, such as type of polyelectrolyte and the charge ratio of the anionic-to-cationic polymers, temperature and concentration [8]. For PIC micelles or nanoparticle, the ionic strength of the solution is a key parameter for stability because of the shielding effect of the ionic species on the electrostatic interactions [9]. Therefore, destabilization of PIC under physiological conditions limits their applications as a drug carrier. It is expected that the hydrophobically modified polyelectrolyte will act to stabilize the PIC nanoparticle by hydrophobic interactions [10]. In our study, ionically cross linked polymeric nanoparticles (ICPNP) fabricated by the one of negative charge polymer and second one by positively charged copolymer or hydrophobically modified polymer (amphiphilic nature) have been explored as excellent drug carrier system. In general, these amphiphilic copolymers consisting of hydrophilic and hydrophobic segments are capable of forming self-assembled polymeric structures in aqueous solutions *via* hydrophobic interactions [11]. These self-assembled nanoparticles are composed of an inner core of hydrophobic moieties and an outer shell of hydrophilic groups. The AmB can easily get incorporated in hydrophobic core of these nanoparticles.

AmB is the first line treatment in VL and is highly effective against various *leishmania* species, but it has severe toxicity problems like hematotoxicity which occurs in around 80% cases and renal tubular damage at therapeutic doses have often limited its clinical applications [12]. The toxicity of AmB during formulation development is of major concern. The toxicity of AmB can be decreased by three ways, first is targeting towards macrophages [13,14], secondly, use of lipids in the formulation (such as Ambisome®, Abelcet®), but they gives costly formulation and thirdly, desired tissue localization, biodistribution and molecular organization of AmB in formulation. In this study, we have prepared and characterized self assembled ICPNP and evaluated for molecular organization, toxicity, macrophage uptake, *in vivo* tissue localization, biodistribution and antileishmanial activity. Here, we used applicability of SA with ICPNP, a drug delivery system for better chemotherapy of VL.

MATERIAL AND METHODS

Materials, Parasites, Cell Lines and Animals

Glycol chitosan (GC, Mw 90 KD, 82.7% degree of deacetylation), sodium alginate, [1-ethyl-3 (dimethylamino) propyl] carbodiimide hydrochloride (EDC), stearic acid, 3-[4, 5-dimethylthiazol-2-yl]-2, 5-diphenyltetrazolium bromide (MTT), and dialysis membrane (MwCO 12 KD) were purchased from Sigma-Aldrich (St. Louis, MO). Dimethylacetamide (DMAc), HPLC grade methanol and acetonitrile were from SD Fine Chem Ltd (Mumbai, India). Amphotericin B (AmB) was kindly provided as a gift sample from Emcure pharmaceutical Ltd. (Pune, India). All other reagents were of analytical grade.

The WHO reference strain of *L. donovani* (MHOM/IN/80/Dd8) was used for both *in vitro* and *in vivo* experiments. *Leishmania* parasites and the macrophage cell line J774A were maintained in RPMI-1,640 medium (Sigma, USA) supplemented with 10% heat inactivated fetal bovine serum (HIFBS), 100 U/ml penicillin and 100 μg/ml streptomycin at 37°C in humidified atmosphere of 5% (v/v) CO_2/air mixture.

Five- to six-week-old Wistar male rats (205 ± 8 g) and Syrian golden male hamsters (*Mesocricetus auratus*, 45–50 g) were used to study the pharmacokinetics and antileishmanial effects of the AmB-formulations, while *in vivo* localization studies, mortality rate and kidney histopathology were performed in male swiss mice (18–20 g) with prior approval of the Animal Ethics Committee of CSIR-Central Drug Research Institute and according to regulations of the Council for the Purpose of Control and Supervision of Experiments on Animals (CPCSEA), Ministry of Social Justice and Empowerment, Government of India. The Indian Animal Ethics Committee (IAEC) approval no. is CDRI/2012/38.

Synthesis of GCS Copolymer

The GCS copolymer was synthesized using EDC coupling method with slight modifications [15]. Briefly, stearic acid (25% with respect to per sugar residue of GC) and EDC (1.2 mol/mol stearic acid) were dissolved in 10 ml ethanol followed by vortexing to get clear solution. This solution was added drop wise in 10 ml aqueous GC solution (0.02 g/ml) under magnetic stirring (Remi, Mumbai, India) for 24 h at room temperature (RT, 25°C). Then the GCS was separated from unreacted stearic acid and EDC using dichloromethane (3×15 ml) followed by lyophilization under freeze dryer.

Preparation of Ionically Cross Linked Polymeric Nanoparticles (SA-GCS-NP)

The SA-GCS-NP was prepared through an ionotropic complexation method. In this method, 2 mg of synthesized copolymer GCS was dissolved in 100 µL of DMAc and added drop wise into 1 ml aqueous phase (distilled water) under 5 min constant stirring followed by vortexing to prepare self assembled GCS. Then 2 mg/ml of SA was added drop wise in self-assembled GCS under magnetic stirring for 30 min followed by size reduction using probe sonicator (Misonix, Berlin, Germany) at 20% amplitude for 180 sec. SA-GCS-NP was optimized from test formulations (F1 to F13) based on concentration of SA, SA to GCS ratio, time and amplitude of sonication as shown in Table I. The optimized formulation was dialyzed against 1,000 ml of water for 24 h using dialysis membrane bag (MwCO 12 KD) for complete removal of free molecules and solvent from this dispersion.

Preparation of AmB Encapsulated SA-GCS-NP

For encapsulation of AmB in SA-GCS-NP, AmB solution (1 mg/100 µL DMAc) was added drop wise in SA-GCS-NP dispersion under stirring, followed by solvent evaporation. For removal of free drug, AmB encapsulated SA-GCS-NP (AmB-SA-GCS-NP) was ultracentrifuged at 40,000×g for 30 min (Thermo scientific, Sorvall, Wx ultra 100, Germany) and obtained pellets were dried under vacuum.

Characterization of SA-GCS-NP

The cumulative mean size and polydispersity index (PDI) of SA-GCS-NP were determined by dynamic light scattering using Zetasizer (Nano ZS, Malvern Instruments, Worcestershire, UK) after suitable dilution in distilled water. All of the measurements were performed in triplicates.

The surface morphology of optimized SA-GCS-NP were ascertained using field emission scanning electron microscopy (FESEM, SUPRA 40VP, Carl Zeiss NTS GmbH, Oberkochen, Germany), and high resolution transmission electron microscopy (HRTEM, Tecnai™ G^2 F20, Eindhoven, The Netherlands) according to our previous publication [4].

Table I Optimization of process parameters in formulation of SA-GCS-NP showing changes in size, polydispersity index and zeta potential and encapsulation efficiency ($n=3$)

Formulation code	Concentration of sodium alginate (% w/v)	Sodium alginate to glycol chitosan stearate ratio	Sonication time (sec)	Sonication amplitude (%)	Size (nm)	Polydispersity index	Zeta potential (mV)	Encapsulation efficiency (% w/w)	Drug loading (% w/w)
F1	0.1	1:2	180	20	248.5 ± 28.3	0.237 ± 0.053	(−) 15.3 ± 4.3	80.23 ± 2.08	22.92 ± 0.59
F2	0.2	1:2	180	20	196.3 ± 17.2	0.216 ± 0.078	(−) 32.4 ± 5.1	89.56 ± 2.91	22.39 ± 0.73
F3	0.3	1:2	180	20	574.2 ± 68.1	0.352 ± 0.102	(−) 41.7 ± 8.4	89.28 ± 2.75	19.84 ± 0.61
F4	0.4	1:2	180	20	684.7 ± 86.4	0.386 ± 0.089	(−) 53.9 ± 13.1	89.17 ± 2.37	17.83 ± 0.48
F5	0.2	1:1	180	20	231.4 ± 23.1	0.232 ± 0.081	(−) 35.2 ± 6.2	87.06 ± 3.59	17.41 ± 0.72
F6	0.2	1:4	180	20	274.6 ± 56.3	0.325 ± 0.094	(−) 27.1 ± 5.6	88.25 ± 4.46	14.70 ± 0.75
F7	0.2	2:1	180	20	408.2 ± 67.5	0.354 ± 0.062	(−) 38.5 ± 7.8	89.18 ± 2.09	12.74 ± 0.29
F8	0.2	4:1	180	20	468.7 ± 74.2	0.410 ± 0.083	(−) 49.7 ± 10.3	89.34 ± 2.87	8.12 ± 0.26
F9	0.2	1:2	60	20	349.7 ± 56.3	0.274 ± 0.078	(−) 31.1 ± 6.8	88.73 ± 3.17	22.18 ± 0.80
F10	0.2	1:2	120	20	288.6 ± 39.8	0.249 ± 0.087	(−) 31.7 ± 5.7	89.12 ± 2.43	22.28 ± 0.61
F11	0.2	1:2	240	20	243.4 ± 37.6	0.207 ± 0.063	(−) 28.3 ± 8.5	88.12 ± 3.46	22.03 ± 0.87
F12	0.2	1:2	180	10	301.8 ± 42.6	0.248 ± 0.084	(−) 31.6 ± 5.4	89.32 ± 2.69	22.33 ± 0.67
F13	0.2	1:2	180	40	261.3 ± 36.8	0.198 ± 0.095	(−) 29.3 ± 7.6	88.75 ± 3.02	22.18 ± 0.76

F1 to F4; Sodium alginate concentration changes while other parameters remain constant

F2, F5 to F8; Sodium alginate to glycol chitosan stearate ratio changes while other parameters remain constant

F2, F9 to F11; Sonication time changes while other parameters remain constant

F2, F12 to F13; Sonication amplitude changes while other parameters remain constant

Determination of AmB Loading and Entrapment Efficiency

The AmB content was determined by extracting the drug from the AmB-SA-GCS-NP using DMAc, diluted with methanol and filtered through 0.45 μm membrane filter and analyzed using HPLC method as described in our previous publication [16]. The percentage of encapsulation efficiency (EE) and drug loading was calculated using following formulae:

$$\text{Encapsulationefficiency} = \text{Wt. of (Total–free)AmB in SA–GCS–NP} \times 100/\text{Wt. of Total AmB}$$

$$\text{Encapsulationefficiency} = \text{Wt. of (Total–free)AmB in SA–GCS–NP} \times 100/\text{Wt. of Total AmB}$$

Tagging of Amphotericin B with FITC (FAmB)

For *in vivo* localization and *in vitro* uptake studies, AmB was tagged with FITC according to previously reported method with slight modifications [14]. In brief, 10 mg of AmB and 5 mg of FITC were dissolved in 2 mL of DMAc followed by addition of 200 μL of triethylamine as base catalyst in 5 mL round bottom flask. The contents were stirred for 2 h at room temperature and thereafter 10 mL ethyl acetate was added to precipitate the compound. Colloidal precipitate was separated by centrifugation at 18,000×g for 10 min and dried over desiccant under vacuum. TLC of the product, AmB and FITC was performed using a mobile phase composed of ethyl acetate: methanol in 2:3 ratios to identify formation of FITC tagged AmB (FAmB).

In Vitro Uptake Study and *In Vivo* Localization in Tissues of AmB-SA-GCS-NP

FAmB was encapsulated in the SA-GCS-NP by solvent injection method followed by solvent evaporation. For this purpose same procedure was followed as described earlier. Briefly, 1 mg of tagged FAmB was dissolved in 100 μL of DMAc and encapsulated drop wise in blank SA-GCS-NP. The J774A cells were placed on to a 12-well cluster dish at a density of 2×10^5 cells/well and cultivated in 800 μL DMEM supplemented with 10% FBS and 1% antibiotic and antimycotic solution. After 24 h the culture medium was replaced with fresh culture medium. FITC tagged formulation (FAmB-SA-GCS-NP) and FAmB at 10 μg/mL concentration were added in well plate containing cells and kept in incubator for 6 h at 37°C and 5% CO_2. After incubation, cells were transferred in vials and relative fluorescence was measured by flow cytometry (Becton Dickinson, Oxford, UK) at λ_{EX} (495 nm) and λ_{EM} (525 nm).

The FITC tagged formulation (FAmB-SA-GCS-NP) and FAmB was administered to mice (n = 3, which is the number of animals taken in one experiment for each formulation) by intravenous route for consecutively 3 days. After 2 h of last dose, the mice were sacrificed and liver, spleen, lung and kidney were isolated, washed with physiological saline, fixed, embedded in wax and sections were made using microtome (LEICA RM 2155, Germany) and photographs were taken using fluorescent microscope (Leica, DMRBE, Bensheim, Germany).

Pharmacokinetic and Biodistribution Study

Analytical Procedures

The HPLC analysis of plasma samples and tissue samples of AmB were carried out using our previously published validated isocratic analytical method [16] using Shimadzu HPLC system equipped with 10 ATVP binary gradient pumps (Shimadzu, Japan), a rheodyne model 7,125 injector (CA, US) with a 20 mL loop and SPD-M10 AVP UV detector (Shimadzu, Japan). The HPLC column [LichroCART® 250–4, Lichrospher® 100, RP-18e, 5 μm, 250×4 mm (Merck KgaA, 64271 Darmstadt, Germany)] and mobile phase [acetonitrile/10 mM KH_2PO_4 buffer, pH 4 (60:40, v/v)] at a flow rate of 1 mL/min was used for analysis of AmB samples. The IKA® T25 digital ULTRA-TURRAX® was used for homogenization of tissues in acetonitrile (1 g of tissue/2 mL of acetonitrile) for 3–4 min over an ice bath. Aliquots of 20 μL of serum and homogenized tissues were used for HPLC analysis. Calibration curves of AmB were linear in the range of 0–10 μg/mL for plasma samples and 0–10 μg/g for tissue samples. The limit of quantification of AmB was 20 ng/mL for plasma samples and 20 ng/g for tissue samples.

Experimental Design

The IV bolus administration of 1 mg/kg AmB-SA-GCS-NP ($n=6$) and 1 mg/kg plain AmB ($n=6$) in 0.2 mL were allocated in two treatment groups. The dose of AmB at which there is clinical nephrotoxicity is reported, was selected for pharmacokinetic and bio-distribution studies. as reported earlier [17]. For minimizing acute toxic effects of AmB, all IV administrations were given slowly and steadily. Systemic blood (0.2 mL) was sampled at 0.5, 1, 2, 3, 5, 8, 12, 24, 48 and 72 h post-dose of IV bolus administrations of AmB-SA-GCS-NP and plain AmB, and withdrawn blood was replaced by an equal volume of normal saline to prevent hypovolaemia. Plasma was separated by centrifugation (2,500 g, 10 min, and 15°C). The animals were sacrificed at 0.5, 1, 2, 3, 5, 8, 12, 24, 48 and

72 h following administration of AmB formulations, and liver, spleen, right lung and right kidney were harvested for drug analysis. Plasma and tissue samples were stored at −80°C until analysis.

In Vitro Anti-Amastigote Assay

The activity of AmB-SA-GCS-NP and plain AmB against intracellular amastigotes was evaluated as per protocol described earlier [18]. Briefly, J774A macrophages (1×10^5 cells/well) in 24-well plates were infected with promastigotes, expressing green fluorescent protein (GFP) at multiplicity of 10 parasites per macrophage. After 12 h incubation 24-well plates were washed thrice with PBS (pH 7.4) to remove non-phagocytosed promastigotes and re-supplemented with RPMI-1640 complete medium, followed by incubation with AmB-SA-GCS-NP and plain AmB at different drug concentrations (10 ng/ml to 5 μg/mL) in triplicate for 48 h. Afterwards, cells were removed, washed and quantitated by flow cytometry equipped with a 20 mW argon laser with excitation at 488 nm and emission at 515 nm followed by multiparametric data analysis by Kaluza analysis software (Beckman Coulter). The parasite growth inhibition was determined by comparing the fluorescence levels of drug-treated parasites with that of untreated control parasites and the 50% and 90% inhibitory concentrations (IC_{50} and IC_{90}) was calculated using GraphPad Prism6.

In Vivo Assay in *L. Donovani* Infected Hamsters

The *in vivo* efficacy of AmB-formulation was evaluated against *L. donovani* amastigotes in a golden hamster model [4]. After 30 days of established infection, male hamsters (n =5 in each group) were intra-peritoneally administered with AmB-SA-GCS-NP and plain AmB having AmB equivalent to 1 mg/kg dose for 5 consecutive days. Treated animals were sacrificed two weeks after treatment and compared with the infected untreated control group. The splenic dab smear of all performed animals, was examined microscopically with the help of Giemsa-stained imprints, in which parasite burdens were calculated by counting the number of amastigotes per 100 macrophage nuclei. The percentage of inhibition (PI) was calculated using the formula:

$$PI = (PP-PT/PP) \times 100$$

Where PP is the number of amastigotes per 100 macrophage nuclei before treatment whereas PT is the number of amastigotes per 100 macrophage nuclei after treatment in spleen.

Toxicity Assay and AmB Molecular Organization in the Formulations

Molecular aggregation state of AmB is directly correlated with toxicity of the drug [4], and it was identified in various formulations using UV-visible spectroscopy (UV-1700 pharmaSpec, shimadzu).

The hemolysis and J774A cell cytotoxicity assay was performed at 5–20 μg/ml AmB concentrations of AmB-SA-GCS-NP, plain AmB and equivalent blank SA-GCS-NP using methods reported previously [16]. Subacute toxicity assay was performed in three mice groups ($n=3$), with AmB-SA-GCS-NP (containing AmB equivalent to 5 mg/kg), plain AmB (1 mg/kg) and saline (control group) administered intravenously having constant volume of 200 μL daily for 15 days. Twelve hours after the last treatment, mice were euthanized and kidney tissues were collected. The kidney tissue samples from control and treated animals were preserved in 10% formalin, embedded in paraffin, sectioned and, stained with haematoxylin and eosin for histopathological examination. In order to assess the acute toxicity of AmB-SA-GCS-NP (5–20 mg/kg) and plain AmB (1–5 mg/kg) were administered in increasing doses to mice groups ($n=6$) by intra-peritoneal route. The animals were examined for mortality over the next 8 h.

Statistical Analysis

All results are presented as mean ± standard deviation (S.D.) of three independent measurements. Statistical significance of differences was analyzed by one-way analysis of variance (ANOVA) and p value of <0.05 was considered significant in all cases.

RESULTS

Preparation and Characterization of SA-AmB-GCS-NP

In the present study, we have used GCS amphiphilic copolymer of GC as hydrophilic shell and stearic acid served as hydrophobic core [4]. This self assembled copolymer (Fig. 1) was found to have enhanced mechanical strength with improved sustained release behavior and stability. The developed formulation using this unique copolymer showed improved intracellular localization and pharmacokinetic profile with reduced toxicity. Additionally this copolymer has ability to induce cytokine release which potentiated its applicability in drug delivery.

The ionotropic complexation method was used to prepare self assembled SA-GCS-NP. This technique represents innovative, cost effective and preferable means for great scalability

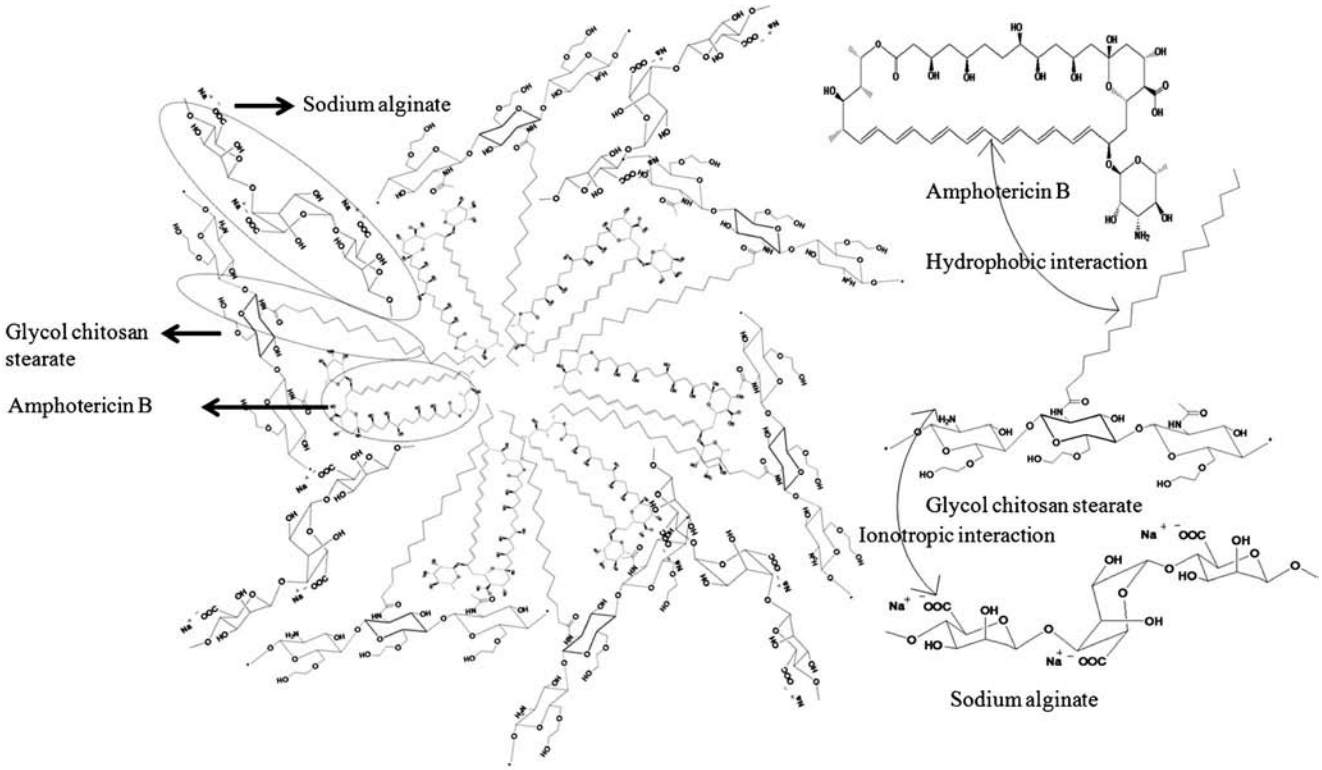

Fig. 1 Schematic representation of self assembled ionically cross linked polymeric nanoparticles

of self assembled copolymer based SA-GCS-NP. Firstly, we prepared copolymer of GCS from GC and stearic acid in the molar ratio of 4:1 through carbodiimide coupling reaction [4]. The prepared GCS copolymer was dissolved in DMAc and this organic solution was added drop wise in aqueous solution of SA over magnetic stirring for 5 min and, subsequently GCS complexes with SA by means of electrostatic interaction between oppositely charged polymeric ions. This process generates self assembled ICPNP. The ICPNP was optimized for particle size, PDI, zeta potential and EE by varying one parameter and keeping other parameters constant as shown in Table I. The variable parameters are concentration of anionic polymer (SA), anionic polymer (SA) to cationic copolymer (GCS) ratio and energy based size reduction parameters such as amplitude and time of sonication. The change in SA concentration (from 0.1 to 0.4% w/w) resulted initial decrease in particle size (from 248.5±28.3 nm to 196.3±17.2 nm) and PDI (from 0.237±0.053 to 0.216±0.078) in case of F1 to F2 respectively, there after rapid growth in size and PDI was observed with F3 and F4 formulation. Beyond SA saturation concentration, it remained uncomplexed with GCS and leads to aggregation in F3 and F4 formulation. The zeta potential increases from (−) 15.3±4.3 to (−)53.9±13.1 mV with increase in SA concentration from F1 to F4 since SA is anionic polymer, while EE initially increases from F1 to F2 (80.23± 2.08 to 89.56±2.91% w/w) thereafter no change in EE was observed (Table I). The increase in SA to GCS ratio from 1:4 to 4:1 causes initial reduction in size and PDI of F2, followed by drastic increase in size and PDI as in case of F5, F7 and F8 formulations while zeta potential increases gradually and EE remains unaltered, This may be attributed to the fact that, beyond certain threshold concentration (0.2% w/v), SA remain uncomplexed and aggregate on SA-GCS-NP that leads to increase in size, PDI and zeta potential. The size reduction process was carried from probe sonicator which affect size and PDI of SA-GCS-NP while other parameters remain similar. As shown in Table I, sonication for 180 sec at 20% amplitude was found to be optimum to achieve the desired size range of SA-GCS-NP with monodisperse population. Although, on increasing sonication time and amplitude, due to development of surface charges on the particles aggregation was observed [19]. In the present experimental set up the optimized parameters for formulation F2 was 0.2% w/v of SA using SA:GCS ratio (1:2) sonicating for 180 seconds to get a particle size of 196.3±17.2 nm. The zeta potential and entrapment efficienct (EE) was found to be (−) 32.4± 5.1 mV and 89.56±2.91% respectively. In case of F9 and F10 the sonication time was 60 and 120 seconds which was probably not sufficient enough to reduce the size to desired range. While, in case of F11 the sonication time of 240 seconds exceeds threshold limit where particles gets aggregated due to production of high instant energy and charge. This

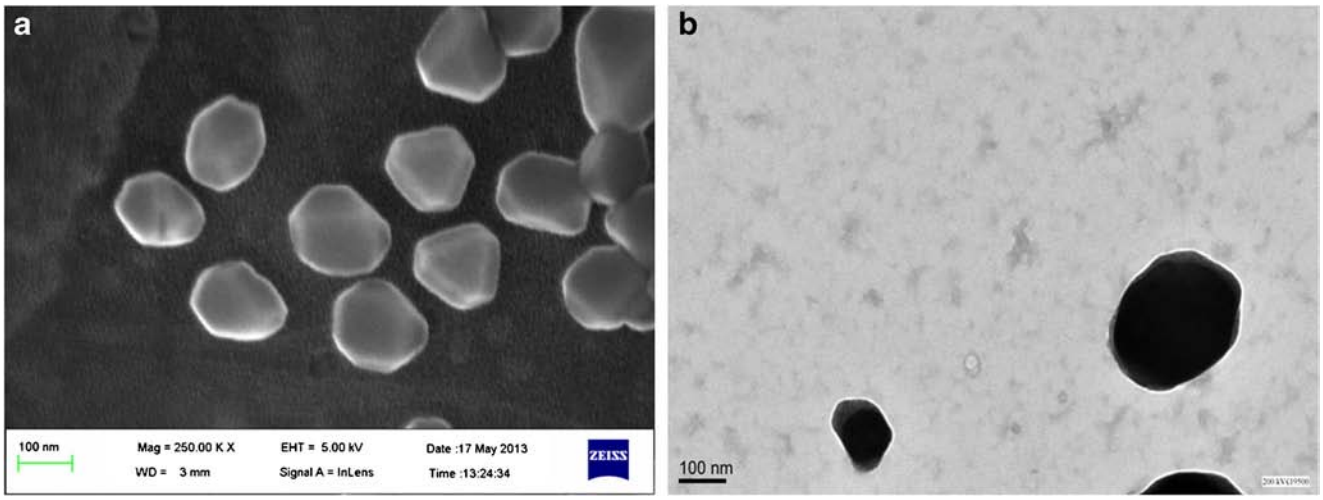

Fig. 2 (**a**) FESEM (Field Emission Scanning Electron Microscopy) and (**b**) HRTEM (High Resolution Transmission Electron Microscopy) micrographs of optimized SA-GCS nanoparticles. The crystal structure present due to polymer ion cross linking and sodium alginate cross linking was observed as a layering over GCS.

could be the reason for getting smallest particle size in case of F2.

Figure 2 shows the morphological characteristics of the SA-GCS-NP by FESEM and HRTEM. The FESEM shows nanocrystal morphology of SA-GCS-NP. The SA layer over GCS was observed as thick covering in HRTEM confirms successful formation of ICPNP as shown in Fig. 2.

In Vitro Uptake and *In Vivo* Tissue Localization of FAmB-SA-GCS-NP

AmB is not inherently fluorescent in visible light, thus, AmB was tagged with FITC (FAmB) and entrapped in SA-GCS-NP. FAmB was characterized using TLC where RF value was slightly higher than AmB and far less than FITC. FAmB was encapsulated in the SA-GCS-NP by solvent injection method and free FAmB was removed by centrifugation and washing.

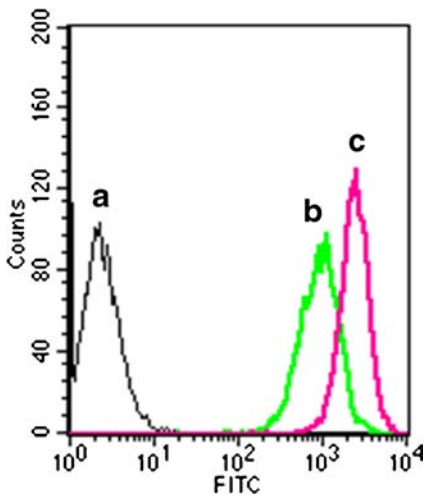

Fig. 3 *In vitro* uptake study of (**a**) control, (**b**) FAmB and (**c**) FAmB-SA-GCS-NP on J774A macrophage cell lines after 6 h incubation.

The *in vitro* uptake of FAmB-SA-GCS-NP (mean fluorescence intensity ~ 496.04) was higher (~1.7) compared to FAmB (mean fluorescence intensity ~278.45) in relative concentration as shown in Fig. 3. *In vivo* tissue localization of FAmB and FAmB-SA-GCS-NP was observed by visualizing intensity of fluorescence in the fluorescence photomicrographs of the liver, lung, spleen and kidney tissues (Fig. 4). The fluorescence observed in the case of FAmB in liver, lung and spleen sections (Fig. 4b) was relatively lower than the fluorescence intensity of the FAmB-SA-GCS-NP (Fig. 4a) while fluorescence intensity was higher in kidney section of FAmB compare to FAmB-SA-GCS-NP.

Pharmacokinetic Profile and Tissue Distribution of AmB-Formulations Following IV Bolus Administration

The AmB-SA-GCS-NP and plain AmB demonstrated statistically significant differences in pharmacokinetics of AmB following IV administration as shown in Fig. 5 and Table II. The IV administration of AmB-SA-GCS-NP resulted in lower concentration of AmB in plasma as compared to plain AmB. However, AmB concentration following IV administration of AmB-SA-GCS-NP was detected till 72 h (Fig. 5). The AUC, MRT, volume of distribution and $t_{1/2}$ was higher following IV administration of AmB-SA-GCS-NP as compared to plain AmB while clearance was decreases as showed in Table II.

The tissue distribution results of AmB-SA-GCS-NP and plain AmB at different time points *i.e.* 0.5, 1, 2, 3, 5, 8, 12, 24, 48 and 72 h following IV administration has been shown in Fig. 5. Significantly higher concentration of AmB was accumulated in the liver and spleen following IV administration of

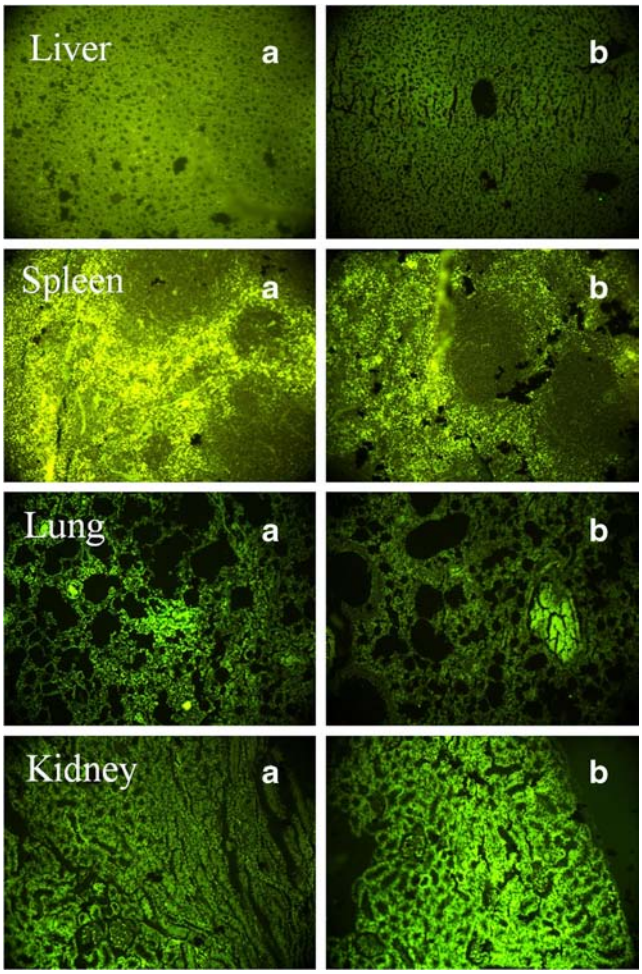

Fig. 4 *In vivo* tissue localization of FITC tagged (**a**) FAmB-SA-GCS-NP and (**b**) FAmB in liver, spleen, lung and kidney following iv administration of AmB equivalent 1 mg/kg daily for consecutively 3 days. The tissues were harvested after 2 h of last IV administration of drug.

AmB-SA-GCS-NP compared to plain AmB ($p<0.05$). However, AmB-SA-GCS-NP showed significantly ($p<0.05$) less distribution in kidney compared to plain AmB. The lung showed increased accumulation of AmB following IV administration of AmB-SA-GCS-NP compared to plain AmB ($p<0.01$).

Inhibitory Effect on *L. Donovani* Intra-Macrophage Amastigotes and *In vivo* Antileishmanial Activity

Inhibitory effect on *L. donovani* has been represented as IC_{50} as well as IC_{90} (Fig. 6(a)). It has been observed that IC_{50} value of AmB-SA-GCS-NP and plain AmB was 0.128 ± 0.024 and 0.214 ± 0.06 μg/mL ($p<0.05$), respectively. The *in vivo* experiment results as shown in Fig. 6(b) clearly revealed that AmB-SA-GCS-NP was significantly more effective ($70.21\pm3.46\%$ inhibition) as compared to plain AmB ($53.24\pm2.84\%$ inhibition) ($p<0.05$) while blank SA-GCS-NP had $9.35\pm0.57\%$ parasite inhibition.

Molecular Organization of AmB and Toxicity Assay of the Formulations

The molecular states of AmB in tested formulation are shown in the Fig. 7(i). The ratio of aggregated/monomeric, represented by ratio of first (346 nm) to the fourth (408 nm) peaks, I/IV (A_{346}/A_{408}), in UV spectrum, which enables analysis of molecular organization and using this ratio, the degree of aggregation of AmB was calculated [20]. As shown in Fig. 7(i(a)), plain AmB shows aggregated/monomeric ratio >2 that indicates presence of aggregated forms of AmB, particularly dimeric [21]. Whereas, A_{346}/A_{408} ratio for AmB-SA-GCS-NP was less than 2 as shown in Fig. 7(i(b)), indicated the presence of monomeric AmB.

Prepared AmB-SA-GCS-NP and SA-GCS-NP exhibited hematotoxicity upto $14.41\pm0.76\%$ and $1.16\pm0.29\%$ whereas plain AmB showed hematotoxicity upto $73.5\pm1.08\%$ as shown in Fig. 7ii(a). The cytotoxicity (reversal of % cell viability) induced by various concentrations of AmB-SA-GCS-NP was less than 5% while plain AmB caused ~30% cytotoxicity in J774A cell line as shown in Fig. 7ii(b). Acute toxicity results suggest that only 16.66% death of mice was found in dose upto 20 mg/kg in case of AmB-SA-GCS-NP. The mortality in mice was 33.33% and 100% at the dose of 2 and 5 mg/kg of plain AmB respectively. (Fig. 7ii(c)). The histopathological analysis of kidney tissue revealed a normal pattern in all treated groups (Fig. 7ii(d,e)) except the plain AmB group, which showed patchy tubular epithelial necrosis that varied in extent from focal to extensive as shown in Fig. 7ii(f).

DISCUSSION

The AmB has major limitation in clinical therapeutics due to its toxicity that was conquered by encapsulating AmB in ICPNP formulation. The ICPNP was prepared by using electrostatic interaction between negatively charged SA polymer and a positively charged GCS copolymer as shown in Fig. 1. This ICPNP has ability to self assemble in aqueous phase due to hydrophilic and hydrophobic segments present in GCS copolymer [4]. The zeta potential of nanoparticle was negative that represents SA occurrence on outer surface of polymeric nanoparticle (Fig. 1). This nanoparticle composed of SA and GCS copolymer has four distinct functions: i) the SA and GCS part of ICPNP restricts conversion of AmB molecular forms from monomeric to multimeric thus reduces toxicity of the AmB; ii) the ICPNP provides desired localization and biodistribution of AmB in tissues; iii) the ICPNP provides stability to formulation and improved sustained release of drug; iv) the SA in outer surface of ICPNP have ability to induce various proinflammatory cytokines and chemokines through macrophage activation [7].

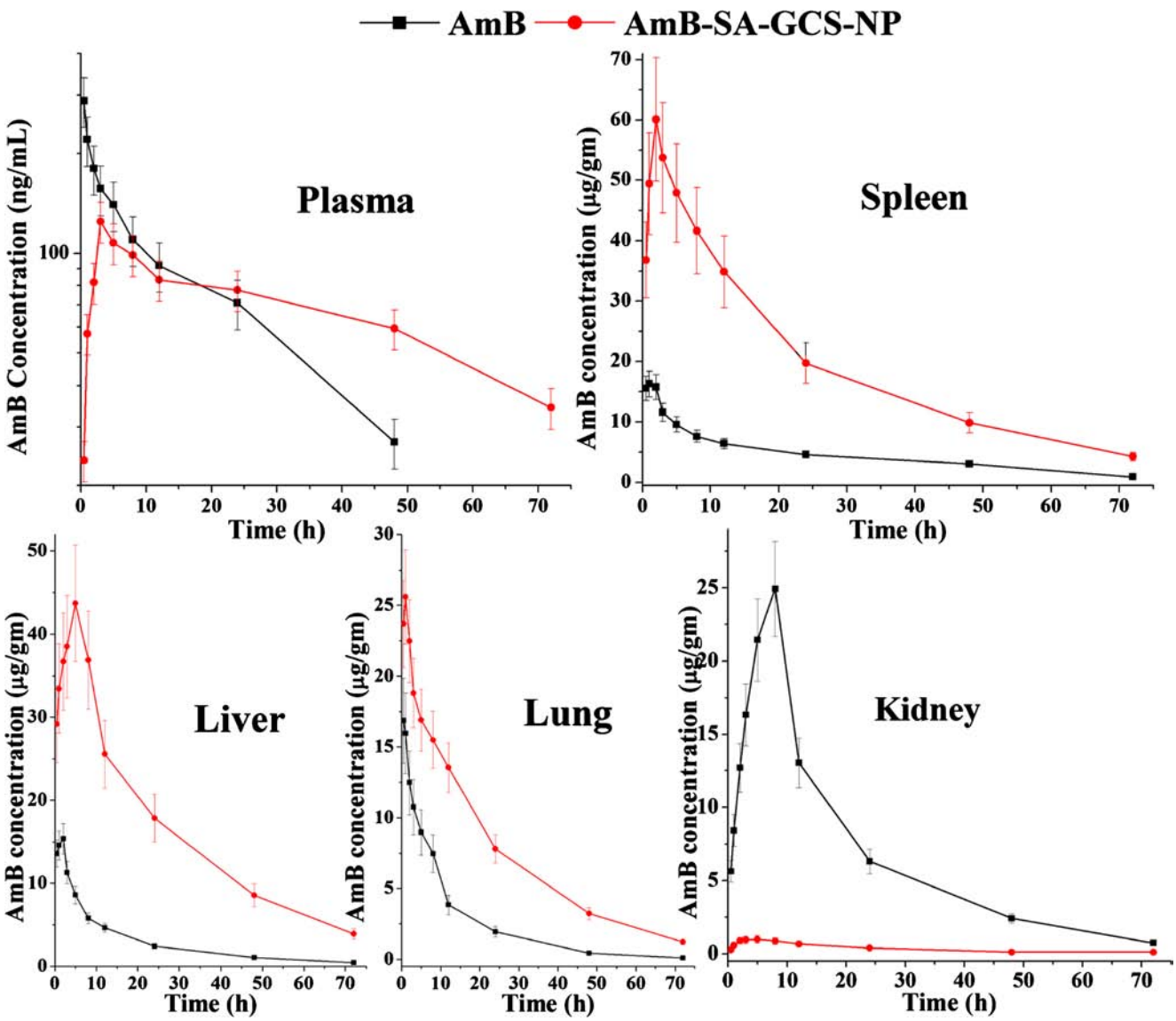

Fig. 5 Plasma AmB concentration-time semi-logarithmic plot (mean ± SEM), Liver, Spleen, Lung and Kidney AmB concentration-time plot (mean ± SEM), following IV bolus administration of AmB-SA-GCS-NP 1 mg/kg and plain AmB 1 mg/kg ($n = 3$).

There are many reports about PIC nanoparticles, but in the present study we have prepared self assembled copolymer based ICPNP. The GC was first conjugated with stearic acid in a molar ratio of 4:1 to form GCS copolymer [4] that has positive zeta potential measured by zeta sizer on its surface that was referred as cationic copolymer. The GCS binds strongly with SA due to strong electrostatic interaction as well as diffusion in SA gel networks [22]. Fabricated SA-GCS-NP has negative surface charge measured by zeta sizer, owing to the presence of SA on outer surface. SA provides elasticity and mechanical strength to polyanion-polycation complex membrane [23]. The strength of interaction and the stability of the

Table II Pharmacokinetic parameters of AmB formulations

AmB equivalent concentration in formulation	$AUC_{0\text{-}72h}$ (hr × ng/ml)	$t_{1/2}$ (hr)	$MRT_{0\text{–}72}$ (hr)	CL (ml/hr/kg)	Vd (ml/kg)
AmB-SA-GCS-NP 1 mg/kg	4,835 ± 681	44.8 ± 5.6	29.8 ± 6.2	141.8 ± 9.8	9,168 ± 629
Plain AmB 1 mg/kg	3,764 ± 526	17.7 ± 2.6	15.9 ± 4.1	227.1 ± 21.8	5,815 ± 527

Each data represents the mean ± standard deviation ($n = 3$)

AUC Area under the curve, $t_{1/2}$: Half life, *MRT* Mean residence time, *CL* Clearance, *Vd* Volume of distribution

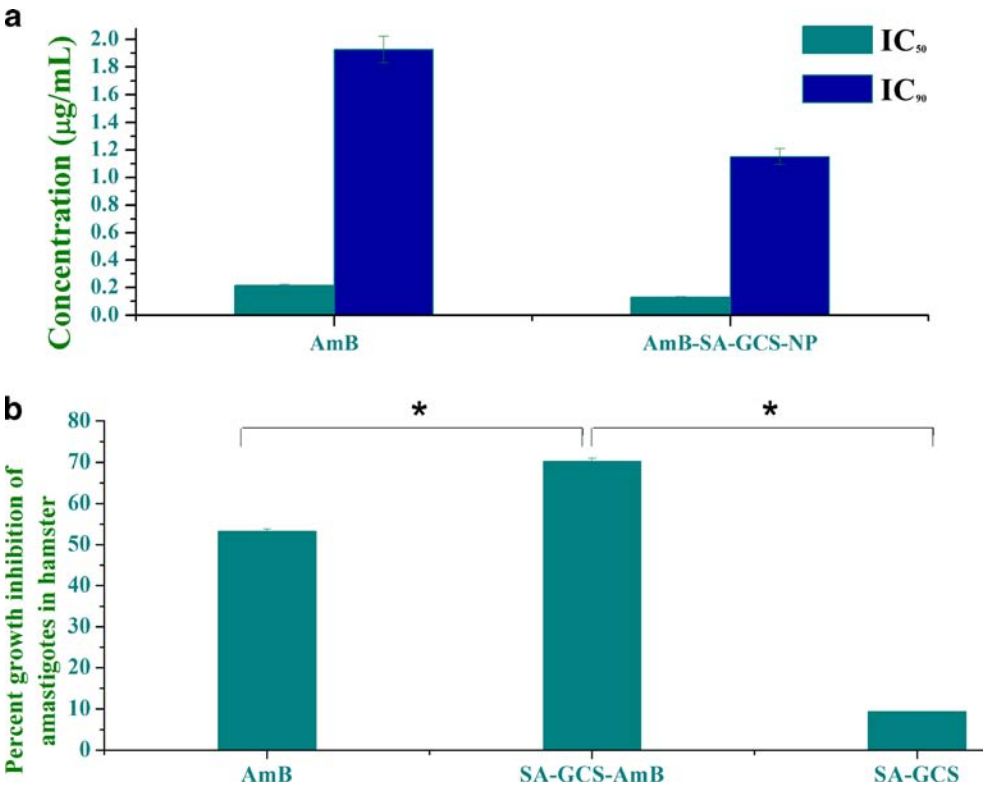

Fig. 6 (**a**) *In vitro* antileishmanial activity (IC_{50} and IC_{90}) of AmB-SA-GCS-NP and plain AmB in *L. donovani* amastigote infected macrophages observed after 48 h of incubation ($n = 3$) (**b**) *In vivo* antileishmanial activity of AmB-SA-GCS-NP and AmB in the established Syrian golden hamster model infected with *L. donovani* amastigotes at an intra-peritoneal dose of 1 mg of AmB/kg body weight of hamster and formulations without drug were injected intra-peritoneally into each hamster on day 31 post-infection. The parasite burden was estimated by splenic biopsy on day 15 post-treatment and percentage parasite inhibition was calculated in comparison with the parasite burden of untreated infected animals (means ± SD) ($n = 5$). The mean parasite burden in the spleen of untreated, infected control animals was 454 ± 38 amastigotes per 100 cell nuclei of macrophages. ($n = 5$) * $p < 0.05$ (comparison of AmB-SA-GCS *versus* AmB and AmB-SA-GCS *versus* SA-GCS).

polyanion-polycation complexes strongly depend on molecular parameters such as chemical composition, sequential structure, conformations and molecular size of both SA and GCS that was observed by nanoparticle size, PDI, zeta potential and encapsulation efficiency of ICPNP as shown in Table I. This characteristics of SA-GCS-NP provides ICPNP, stability and sustained release of drug in physiological conditions [23]. The SA-GCS-NP has crystal shape as observed in FESEM and SA present as surface layering in SA-GCS-NP as shown in HRTEM (Fig. 2). Thus, it confirms presence of SA on the surface of SA-GCS-NP. Due to crystal nature of ICPNP, excellent performance is anticipated *in vivo*, like improvement in bioavailability, potential site-specific drug delivery and reduced toxicity of the formulation.

Previously, our group has reported that SA decorated nanocapsules containing doxorubicin induces macrophage cells to secrete inflammatory cytokines and chemokines [7]. In continuation to this, we have demonstrated that SA in ICPNP would prominently reduce AmB mediated toxicity evaluated by *in vivo* localization study, pharmacokinetics and biodistribution profile of AmB encapsulated ICPNP, and on the other hand, ICPNP restricts molecular conversion of AmB in aggregated multimeric forms which helps in reducing possible side effects of AmB.

The particulate drug delivery systems easily get engulfed by macrophages through phagocytosis [24,25]. The tagged FAmB-SA-GCS-NP shows significantly higher uptake (~1.7) ($p < 0.05$) in contrast to tagged FAmB in J774A macrophagic cell lines (Fig. 3) demonstrating superior uptake of tagged FAmB-SA-GCS-NP delivery system over tagged FAmB, was also observed by greater localization of fluorescence in macrophage rich organs liver, spleen and lung (Fig. 4), which was also supported by previous work [26,27]. The mechanism behind higher uptake was facilitated by adhesion of tagged FAmB-SA-GCS-NP to the macrophage cell membrane due to sodium alginate's biological adhesion properties followed by internalization process compared to tagged FAmB in macrophages. It is also reported that lipid-raft-dependent and clathrin mediated endocytosis by macrophages is evident for efficient uptake of particles [28,29]. While tagged FAmB-SA-GCS-NP has lesser localization in kidney tissues which was concurrent with previous studies as particle size, shape and charge has no role in drug localization in kidney [30] and leads to reduction in AmB associated nephrotoxicity. The tagged FAmB shows higher fluorescence in kidney tissues

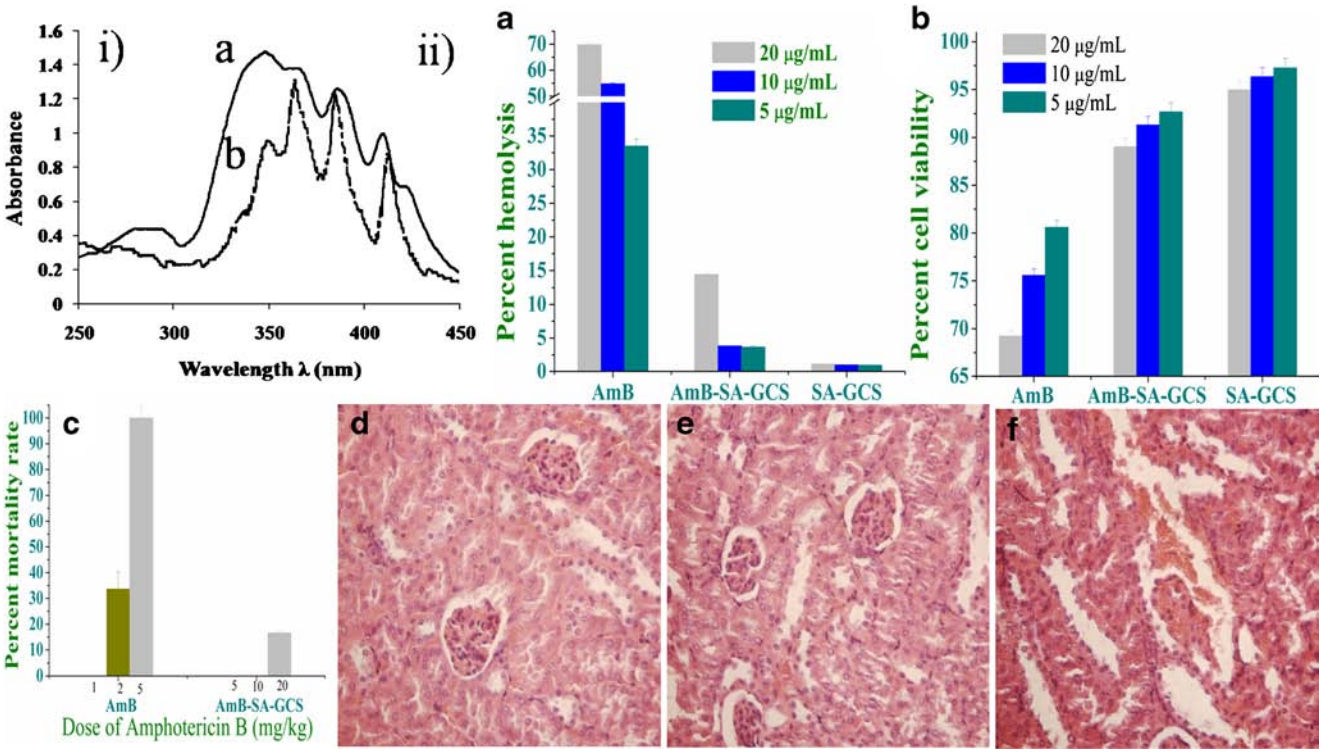

Fig. 7 *i*) Molecular organization of AmB in different formulations (**a**) AmB and (**b**) AmB-SA-GCS-NP (10 µg/ml) from UV-visible spectroscopy. *ii*) The effect of AmB-SA-GCS-NP and AmB equivalent to Amphotericin B concentration of 5, 10 and 20 µg/mL on (**a**) RBCs collected from Wistar rat's blood (b) J774A macrophage cell line ($n = 3$). (**c**) Percent mortality rate of six mice group ($n = 6$) treated with AmB (1, 2, 5 mg/kg), AmB-SA-GCS-NP (5, 10, 20 mg/kg) through intra-peritoneal route. Histopathology of kidney from treated mice after iv dose of (**d**) Control group; normal saline, (**e**) AmB-SA-GCS-NP group; 5 mg AmB/kg and (**f**) AmB group; 1 mg AmB/kg.

due to higher drug excretion from body which results toxicity of AmB.

The desired localization and macrophage uptake of the AmB-SA-GCS-NP as compared to plain AmB was also supported by pharmacokinetics and biodistribution study of AmB-SA-GCS-NP as showed in Fig. 5. Basically, distribution relay on type of carrier system (polymer structure, particle size, shape, charge and configuration) which can carry drug molecule to the desired tissue compartments, accordingly drug in carrier system and free drug showed altered pharmacokinetics and bio-distribution profile. It is well known that the structured vehicle especially polymeric systems like AmB-SA-GCS-NP with particle size nearly 200 nm, . are recognized by MPS system and are preferentially taken up by liver spleen and lungs exactly where the drug is desired for the conditions of leishmaniasis. Moreover, this formulation can hold the drug for relatively longer time and release the drug in sustained manner. Similar is the case with our formulation. Sustained release fraction that binds with lipoprotein cleared from body nearly 15 days later [31]. This resulted in faster clearance of plain AmB as compared to AmB-SA-GCS-NP (Table II). The AmB-SA-GCS-NP facilitated uptake of AmB in MPS organs and anticipate that AmB remains in tissues for prolonged period of time once reached [32,33], followed by redistribution of drug in to the blood stream as observed in other lipid-based AmB formulations with similar pharmacokinetic behavior [34] and subsequent slow elimination from the body. The AmB get more concentrated in the liver and spleen when administered with AmB-SA-GCS-NP due to the nanoparticulate and crystal nature [35,36] of the formulation while plain AmB showed relatively lower concentration in liver and spleen (Fig. 5). As we can see in Fig. 5 the maximum concentration of AmB in kidney was found to be almost 25 µg/gm when plain AmB was administered while with AmB-SA-GCS-NP it was less than 2.5 µg/gm which is almost 10 times less than plain AmB. Higher uptake in spleen and liver is also evident in Fig. 5 as maximum concentration of AmB was nearly 60 and 45 µg/gm respectively. . This data clearly shows preferential uptake in spleen and liver. Amphotericin B has been reported to causes severe renal vasoconstriction and can reduce the glomerular filtration rate (GFR) by more than half. Amphotericin B interact directly with cell membrane and increase permeability, as well as induces activation of intrarenal mechanisms (tubuloglomerular feedback) and/or release of mediators (thromboxane A2) and results in nephrotoxicity [37]. The latter effects are possibly responsible for the observed acute decrease in renal blood flow and filtration rate. This clearly indicates that toxicity in the kidney could be reduced to greater extent using AmB-SA-GCS-NP This data is in

accordance with our previous report [17,35] which states that AmB is more nephrotoxic than lipid based formulation..

Figure 5 and Table II showed enormous difference between observed drug concentration and calculated pharmacokinetic parameters of plain AmB and AmB-SA-GCS-NP in plasma. AmB-SA-GCS-NP showed lower plasma drug concentrations than the plain AmB. This suggests a slower release rate as a result of the higher rigidness and molecular interaction with SA and GCS, which may delay release of AmB in a rat model. The AmB from AmB-SA-GCS-NP could be detected till 72 h of IV administration because of sustained plasma level and decreased clearance of drug which represents non-linear saturation like kinetic profile. The AUC, MRT and $t_{1/2}$ of IV administered AmB-SA-GCS-NP was higher compared with the plain AmB (Table II) due to complex pharmacokinetics of AmB-SA-GCS-NP which helps in clinical therapeutics of AmB due to reduction of AmB related toxicities [14]. This was supported by previous reports suggested that different components of AmB formulations, such as poloxamer 188 or poly (caprolactone) [38] and polyethylene glycol-poly lactic acid based polymerosomes [36], affect the distribution characteristics of the drug in the body. Furthermore, it is well known that *Leishmania* parasites mainly resides in macrophages of spleen and liver which is a desired localization. The pharmacokinetics and biodistribution of drug in liver and spleen tissues may be helpful in complete eradication of parasites from this infected organs more efficiently.

Constructively, higher biodistribution of AmB in liver and spleen when administered in the form of AmB-SA-GCS-NP and cytokine inducing property of SA [7], synergistically enhanced *in vitro* and *in vivo* antileishmanial activity of AmB-SA-GCS-NP compared to plain AmB ($p<0.05$) as shown in Fig. 6.

Furthermore, AmB-SA-GCS-NP reduces toxicity of AmB by restricting its conversion from monomer to aggregated form. It has been reported that AmB in aggregated structure can only form ion channels *via* pore formation in a membrane that is responsible for toxicity towards mammalian cells [12,39]. The AmB aggregate generation depends on formulation aspect while AmB is known to assemble in different forms at molecular level such as monomeric, dimeric and multimeric or these forms can coexist. As shown in Fig. 7(i), the spectral modifications induced by aggregation may be represented by the ratio of A_{346}/A_{408}, is indicative of the aggregated/monomeric ratio which enables analysis of formation of molecular forms and by using this ratio, degree of aggregation of AmB can be designed [20]. As calculated from Fig. 7(i(a)), plain AmB has aggregated/monomeric ratio value >2 which indicates the presence of aggregated forms of AmB, particularly dimeric, consistent to previous reports [21]. Whereas, A_{346}/A_{408} ratio for AmB-SA-GCS-NP was less than 2 as calculated from Fig. 7(i(b)), indicates the presence of monomeric AmB. The stearic acid domain in AmB-SA-GCS-NP prevents self-association of monomeric AmB molecules due to strong interaction among SA polymer, GCS copolymer and AmB, thus reduced the aggregated forms [3]. Fig. 7(ii(a),(b)) shown that plain AmB has very high hemolysis and cell cytotoxicity on Wistar rat RBCs and J744A cell lines, respectively even at low doses due to presence of multimeric and aggregated form of AmB present while AmB-SA-GCS-NP was relatively less toxic owing to monomeric form of AmB. This is an agreement with previous reports that the aggregated form of AmB is more toxic against human erythrocytes and other cultured mammalian cells than the monomeric form of the drug [40]. Mice group injected with AmB-SA-GCS-NP illustrated more tolerance to the AmB as revealed from results that mice group can tolerate drug up to 20 mg/kg. On other side, plain AmB treated mice group showed 100% mortality only at 5 mg/kg dose as shown in Fig. 7ii(c) that restricts further increase in plain AmB dose. This was further supported by histopathological analysis of kidney tissue revealed a normal pattern in control and AmB-SA-GCS-NP groups (Fig. 7(ii(d,e))) except the AmB group, which showed patchy tubular epithelial necrosis that varied in extent from focal to extensive (Fig. 7(ii(f))). It was well reported that AmB frequently causes nephrotoxicity also showed in our results while our formulation AmB-SA-GCS-NP was safe and diminished nephrotoxicity even at higher doses since of monomeric form of AmB present in formulation.

The lipid based formulations of AmB are unstable in nature and very high cost of treatment urge to concern in its use as a therapeutic agent, and represent a limitation to widespread use in poor countries. Hence, desired localization and biodistribution in spleen and liver tissues, immunomodulatory property of SA in formulation effectively synergizes killing of *L. donovani* parasites from AmB-SA-GCS-NP and reduced toxicities of formulation after parenteral administration made possible to achieve most favorable therapeutic effect. Furthermore, the excipients and process used in preparation of AmB-SA-GCS-NP formulation was very economical compared to lipid based marketed formulations.

CONCLUSION

The AmB-SA-GCS-NP is novel and simple drug delivery system. The results in this study demonstrated that there is relationship between localization, uptake, biodistribution, activity and toxicity of the sodium alginate cross linked ICPNP formulation. The ICPNP restricts conversion of AmB in monomeric to aggregated forms leading to reduced drug related toxicities. In equivalent doses, our AmB-SA-GCS-NP formulation was effective in parasite clearance with widely spaced and biologically safe therapeutic regimen. Hence, present

work clearly suggests, that ICPNP is therapeutically applicable AmB delivery approach for safer and cost effective chemotherapy of visceral leishmaniasis.

ACKNOWLEDGMENTS AND DISCLOSURES

P.K.G. thankfully acknowledges CSIR, New Delhi, India for awarding fellowship. Authors are thankful to Electron Microscope Facility at Department of Anatomy, All India Institute of Medical Sciences (AIIMS, New Delhi, India) for providing electron microscope analysis. The authors also thank financial support from CSIR network project BIOCERAM (ESC 0103).The CDRI communication number of this manuscript is 8852.

REFERENCES

1. Carvalho EM, Barral A, Pedral-Sampaio D, Barral-Netto M, Badaro R, Rocha H, *et al.* Immunologic markers of clinical evolution in children recently infected with Leishmania donovani chagasi. J Infect Dis. 1992;165(3):535–40.
2. Uchegbu IF, Sadiq L, Arastoo M, Gray AI, Wang W, Waigh RD, *et al.* Quaternary ammonium palmitoyl glycol chitosan–a new polysoap for drug delivery. Int J Pharm. 2001;224(1–2):185–99.
3. Adams ML, Kwon GS. Relative aggregation state and hemolytic activity of amphotericin B encapsulated by poly(ethylene oxide)-block-poly (N-hexyl-L-aspartamide)-acyl conjugate micelles: effects of acyl chain length. J Control Release. 2003;87(1–3):23–32.
4. Gupta PK, Jaiswal AK, Kumar V, Verma A, Dwivedi P, Dube A, *et al.* Covalent functionalized self-assembled lipo-polymerosome bearing amphotericin B for better management of leishmaniasis and its toxicity evaluation. Mol Pharm. 2014;11(3):951–63.
5. Yoshioka T, Skalko N, Gursel M, Gregoriadis G, Florence AT. A non-ionic surfactant vesicle-in-water-in-oil (v/w/o) system: potential uses in drug and vaccine delivery. J Drug Target. 1995;2(6):533–9.
6. Singodia D, Khare P, Dube A, Talegaonkar S, Khar RK, Mishra PR. Development and performance evaluation of alginate-capped amphotericin B lipid nanoconstructs against visceral leishmaniasis. J Biomed Nanotechnol. 2011;7(1):123–4.
7. Kansal S, Tandon R, Verma A, Misra P, Choudhary AK, Verma R, *et al.* Coating doxorubicin-loaded nanocapsules with alginate enhances therapeutic efficacy against Leishmania in hamsters by inducing Th1-type immune responses. Br J Pharmacol. 2014;171(17): 4038–50.
8. Hartig SM, Greene RR, DasGupta J, Carlesso G, Dikov MM, Prokop A, *et al.* Multifunctional nanoparticulate polyelectrolyte complexes. Pharm Res. 2007;24(12):2353–69.
9. Jaturanpinyo M, Harada A, Yuan X, Kataoka K. Preparation of bionanoreactor based on core-shell structured polyion complex micelles entrapping trypsin in the core cross-linked with glutaraldehyde. Bioconjug Chem. 2004;15(2):344–8.
10. Hu FQ, Wu XL, Du YZ, You J, Yuan H. Cellular uptake and cytotoxicity of shell crosslinked stearic acid-grafted chitosan oligosaccharide micelles encapsulating doxorubicin. Eur J Pharm Biopharm. 2008;69(1):117–25.
11. Gaucher G, Dufresne MH, Sant VP, Kang N, Maysinger D, Leroux JC. Block copolymer micelles: preparation, characterization and application in drug delivery. J Control Release. 2005;109(1–3):169–88.
12. Wasko P, Luchowski R, Tutaj K, Grudzinski W, Adamkiewicz P, Gruszecki WI. Toward understanding of toxic side effects of a polyene antibiotic amphotericin B: fluorescence spectroscopy reveals widespread formation of the specific supramolecular structures of the drug. Mol Pharm. 2012;9(5):1511–20.
13. Singodia D, Verma A, Verma RK, Mishra PR. Investigations into an alternate approach to target mannose receptors on macrophages using 4-sulfated N-acetyl galactosamine more efficiently in comparison with mannose-decorated liposomes: an application in drug delivery. Nanomedicine: NBM. 2012;8(4): 468–77.
14. Gupta PK, Asthana S, Jaiswal AK, Kumar V, Verma AK, Shukla P, *et al.* Exploitation of lectinized lipo-polymerosome encapsulated Amphotericin B to target macrophages for effective chemotherapy of visceral leishmaniasis. Bioconjug Chem. 2014;25(6):1091–102.
15. Nakajima N, Ikada Y. Mechanism of amide formation by carbodiimide for bioconjugation in aqueous media. Bioconjug Chem. 1995;6(1):123–30.
16. Asthana S, Jaiswal AK, Gupta PK, Pawar VK, Dube A, Chourasia MK. Immunoadjuvant chemotherapy of visceral leishmaniasis in hamsters using amphotericin B-encapsulated nanoemulsion template-based chitosan nanocapsules. Antimicrob Agents Chemother. 2013;57(4):1714–22.
17. Boswell GW, Bekersky I, Buell D, Hiles R, Walsh TJ. Toxicological profile and pharmacokinetics of a unilamellar liposomal vesicle formulation of amphotericin B in rats. Antimicrob Agents Chemother. 1998;42(2):263–8.
18. Mookerjee Basu J, Mookerjee A, Banerjee R, Saha M, Singh S, Naskar K, *et al.* Inhibition of ABC transporters abolishes antimony resistance in Leishmania Infection. Antimicrob Agents Chemother. 2008;52(3):1080–93.
19. Jain JP, Kumar N. Development of amphotericin B loaded polymersomes based on (PEG) (3)-PLA co-polymers: Factors affecting size and *in vitro* evaluation. Eur J Pharm Sci. 2010;40(5):456–65.
20. Barwicz J, Christian S, Gruda I. Effects of the aggregation state of amphotericin B on its toxicity to mice. Antimicrob Agents Chemother. 1992;36(10):2310–5.
21. Charvalos E, Tzatzarakis MN, Van Bambeke F, Tulkens PM, Tsatsakis AM, Tzanakakis GN, *et al.* Water-soluble amphotericin B-polyvinylpyrrolidone complexes with maintained antifungal activity against Candida spp. and Aspergillus spp. and reduced haemolytic and cytotoxic effects. J Antimicrob Chemother. 2006;57(2):236–44.
22. Gaserod O, Smidsrod O, Skjak-Braek G. Microcapsules of alginate-chitosan–I. A quantitative study of the interaction between alginate and chitosan. Biomaterials. 1998;19(20):1815–25.
23. Thu B, Bruheim P, Espevik T, Smidsrod O, Soon-Shiong P, Skjak-Braek G. Alginate polycation microcapsules. II. Some functional properties. Biomaterials. 1996;17(11):1069–79.
24. Asthana S, Gupta PK, Chaurasia M, Dube A, Chourasia MK. Polymeric colloidal particulate systems: intelligent tools for intracellular targeting of antileishmanial cargos. Expert Opin Drug Delivery. 2013;10(12):1633–51.
25. Alexis F, Pridgen E, Molnar LK, Farokhzad OC. Factors affecting the clearance and biodistribution of polymeric nanoparticles. Mol Pharm. 2008;5(4):505–15.
26. Tabata Y, Ikada Y. Effect of the size and surface charge of polymer microspheres on their phagocytosis by macrophage. Biomaterials. 1988;9(4):356–62.
27. He C, Hu Y, Yin L, Tang C, Yin C. Effects of particle size and surface charge on cellular uptake and biodistribution of polymeric nanoparticles. Biomaterials. 2010;31(13):3657–66.
28. Simons K, Toomre D. Lipid rafts and signal transduction. Nat Rev Mol Cell Biol. 2000;1(1):31–9.

29. Gupta GK, Kansal S, Misra P, Dube A, Mishra PR. Uptake of biodegradable gel-assisted LBL nanomatrix by Leishmania donovani-infected macrophages. AAPS PharmSciTech. 2009;10(4):1343–7.
30. Reddy LH, Sharma RK, Chuttani K, Mishra AK, Murthy RR. Etoposide-incorporated tripalmitin nanoparticles with different surface charge: formulation, characterization, radiolabeling, and biodistribution studies. AAPS J. 2004;6(3):e23.
31. Chabot GG, Pazdur R, Valeriote FA, Baker LH. Pharmacokinetics and toxicity of continuous infusion amphotericin B in cancer patients. J Pharm Sci. 1989;78(4):307–10.
32. Francis P, Lee JW, Hoffman A, Peter J, Francesconi A, Bacher J, *et al.* Efficacy of unilamellar liposomal amphotericin B in treatment of pulmonary aspergillosis in persistently granulocytopenic rabbits: the potential role of bronchoalveolar D-mannitol and serum galactomannan as markers of infection. J Infect Dis. 1994;169(2):356–68.
33. Smith PJ, Olson JA, Constable D, Schwartz J, Proffitt RT, Adler-Moore JP. Effects of dosing regimen on accumulation, retention and prophylactic efficacy of liposomal amphotericin B. J Antimicrob Chemother. 2007;59(5):941–51.
34. Heinemann V, Bosse D, Jehn U, Kahny B, Wachholz K, Debus A, *et al.* Pharmacokinetics of liposomal amphotericin B (Ambisome) in critically ill patients. Antimicrob Agents Chemother. 1997;41(6):1275–80.
35. Li SD, Huang L. Pharmacokinetics and biodistribution of nanoparticles. Mol Pharm. 2008;5(4):496–504.
36. Jain JP, Jatana M, Chakrabarti A, Kumar N. Amphotericin-B-loaded polymersomes formulation (PAMBO) based on (PEG) (3)-PLA copolymers: an *in vivo* evaluation in a murine model. Mol Pharm. 2011;8(1):204–12.
37. Andes D, Safdar N, Marchillo K, Conklin R. Pharmacokinetic-pharmacodynamic comparison of amphotericin B (AMB) and two lipid-associated AMB preparations, liposomal AMB and AMB lipid complex, in murine candidiasis models. Antimicrob Agents Chemother. 2006;50(2):674–84.
38. Echevarria I, Barturen C, Renedo MJ, Troconiz IF, Dios-Vieitez MC. Comparative pharmacokinetics, tissue distributions, and effects on renal function of novel polymeric formulations of amphotericin B and amphotericin B-deoxycholate in rats. Antimicrob Agents Chemother. 2000;44(4):898–904.
39. Huang W, Zhang Z, Han X, Tang J, Wang J, Dong S, *et al.* Ion channel behavior of amphotericin B in sterol-free and cholesterol- or ergosterol-containing supported phosphatidylcholine bilayer model membranes investigated by electrochemistry and spectroscopy. Biophys J. 2002;83(6):3245–55.
40. Legrand P, Romero EA, Cohen BE, Bolard J. Effects of aggregation and solvent on the toxicity of amphotericin B to human erythrocytes. Antimicrob Agents Chemother. 1992;36(11):2518–22.